Journal of Molecular Structure 1048 (2013) 83–87

Contents lists available at SciVerse ScienceDirect

Journal of Molecular Structure

journal homepage: www.elsevier.com/locate/molstruc

Comparison of hair from rectum cancer patients and from healthy persons by Raman microspectroscopy and imaging ☆

Xiaoli Wei [a,b], Xin Wang [c], Yusheng Fang [b], Qing Huang [a,b,c,*]

[a] Hefei Institutes of Physical Science, Chinese Academy of Sciences, Shushanhu Road 350, Hefei 230031, China
[b] University of Science and Technology of China, Hefei 230031, China
[c] College of Basic Medicine, Anhui Medical University, Hefei 230031, China

HIGHLIGHTS

- Raman spectra of hair from cancer patients show some abnormality.
- Raman imaging provides more details by identifying patient hair micro-structures.
- Raman microspectroscopy and imaging of hair may be useful for cancer diagnosis.

ARTICLE INFO

Article history:
Received 20 March 2013
Received in revised form 18 April 2013
Accepted 3 May 2013
Available online 20 May 2013

Keywords:
Raman spectroscopy
Microspectroscopy and imaging
Hair
Cancer

ABSTRACT

In this work, Raman microspectroscopy and imaging was employed to analyze cancer patients' hair tissue. The comparison between the hair from rectum cancer patients and the hair from healthy people reveals some remarkable differences, such as for the rectum cancer patients, there are more lipids but less content of α-helix proteins in the hair medulla section. Though more statistic data are required to establish universary rules for practical and accurate diagnosis, this work based on case study demonstrates the possibility of applying Raman microspectroscopy to reveal abnormality in non-cancer tissues such as hair in order to predict and diagnose cancers.

1. Introduction

Raman spectroscopy is a powerful tool which has been widely applied in biological and biomedical areas because it can provide characteristic chemical and structural informations of measured bio-samples, and it can be utilized to analyze bio-samples in a convenient and non-invasive fashion [1]. Especially, with the development of Raman microspectroscopy and imaging technology, nowadays it allows to analyze a bio-sample with both chemical composition information and high spatial resolution. Recently, with the encouraging progress in the innovative technology such as optical biopsy, targeted techniques and surface-enhanced Raman spectroscopy (SERS), a new trend emerges as to apply Raman spectroscopy and imaging in medical diagnosis of diseases [2–4]. For example, Raman spectroscopy has been applied for diagnosis diseases on the molecular and cellular levels such as breast cancer [3–6], bladder cancer [7,8], prostate cancer [9,10] and cervical cancer [11].

Cancer is the enemy of human health and millions of people die of cancers each year. Currently, accurate cancer diagnosis mostly depends on biopsy or histopathological examination which requires to retrieve cancer tissue samples from patients' bodies. The sampling for biopsy is inconvenient and normally causes great pains of patients. According to Chinese traditional medicine, however, human tissues such as hair and finger nails can reveal people's health conditions. In this sense, hair and finger nails may also serve as the objects for disease prediction or diagnosis. Actually, some studies have already demonstrated the usefulness of spectroscopy and imaging methods in some biomedical researches and applications based on the analysis of the chemical composition changes in personal hair [12–14]. Inspired by these studies, this work attempted to identify certain cancer diseases by analyzing some cancer patients' hair based on the information obtained from Raman microspectroscopy and imaging. The comparison between

* Corresponding author at: Hefei Institutes of Physical Science, Chinese Academy of Sciences, Shushanhu Road 350, Hefei 230031, China. Tel./fax: +86 551 5595261.
E-mail address: huangq@ipp.ac.cn (Q. Huang).

0022-2860/$ - see front matter © 2013 The authors. Published by Elsevier B.V. All rights reserved.
http://dx.doi.org/10.1016/j.molstruc.2013.05.005

the hair from the cancer patients and the hair from normal people reveals some remarkable differences in the distribution of lipid and protein in the cross-section of hair, suggesting that Raman micro-spectroscopy and imaging of non-cancer tissues may also provide an alternative quick and convenient tool to diagnosis of cancer diseases.

2. Experimental

2.1. Sample preparation

The patient hair was taken from four rectal cancer patients who were hospitalized in the First Affiliated Hospital of Anhui Medical

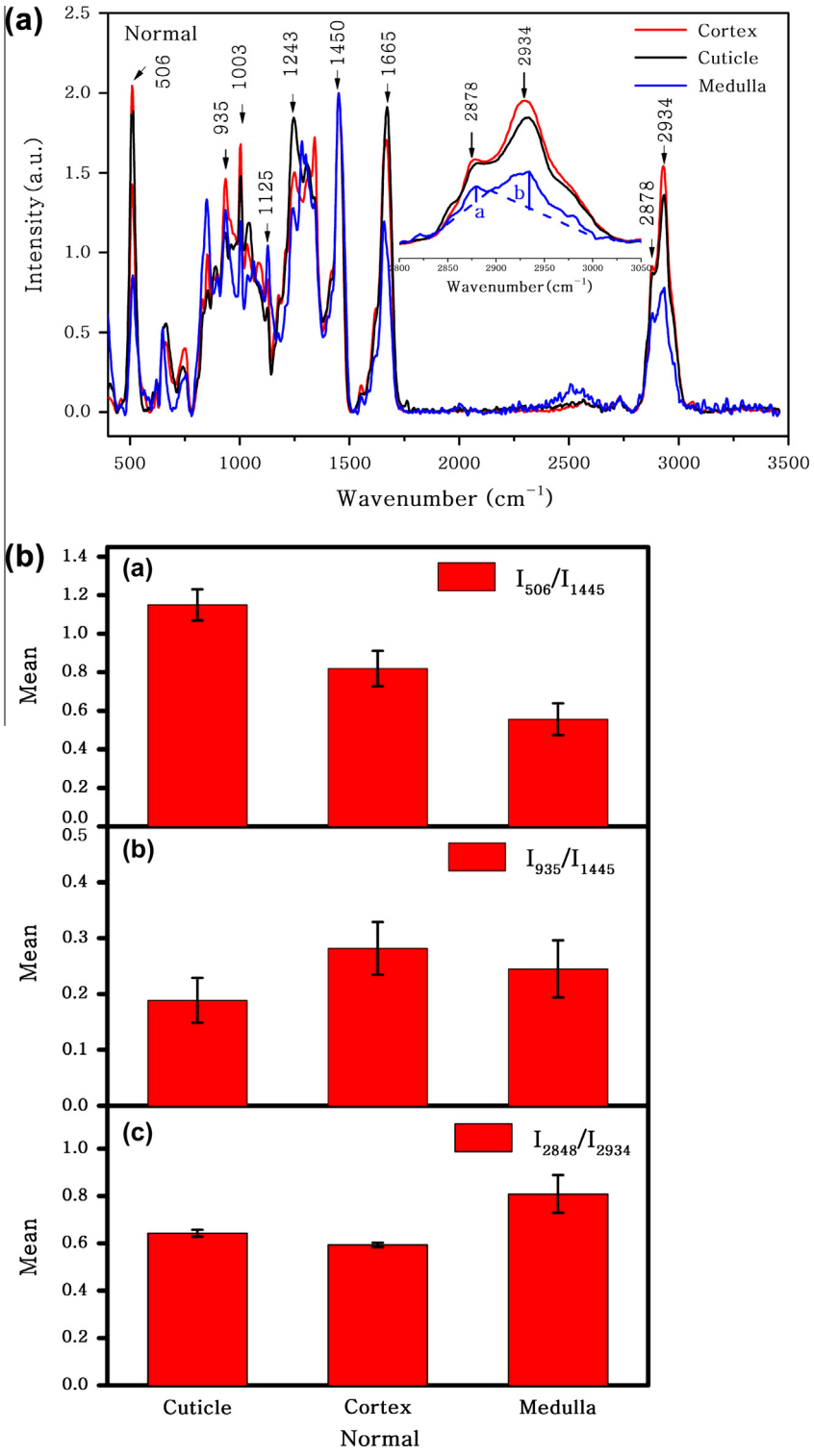

Fig. 1. (a) Raman spectra from the three sections which are normalized at 1450 cm^{-1}. In the hair cross-section, six different locations of each section (medulla, cortex and cuticle) were chosen randomly for collecting spectra. (b) Comparison of the differences for the intensity ratios for I(506 cm^{-1})/I(1445 cm^{-1}), I(935 cm^{-1})/I(1445 cm^{-1}), and I(2848 cm^{-1})/I(2934 cm^{-1}) among three different parts of the normal hair.

Table 1
Assignments of Raman bands of hair[15–22].

Wavenumber (cm^{-1})	Vibrational assignments
506	S–S stretching (gauche–gauche–gauche)
524	S–S stretching (gauche–gauche–trans)
544	S–S stretching (trans–gauche–trans)
935	C–C skeletal stretching (α-helix)
1003	Phenylalanine, symmetric ring stretching
1080	C–C skeletal stretching of random conformation of lipid
1030	Phenylalanine, C–H ring deformation
1125	C–C skeletal stretching of all-trans acyl chain of lipid
1243	Amide III protein random
1450	CH_2 deformation (proteins, lipids)
1652	Amide I (α-helix)
1671	Amide I (β-sheet and random structures)
2848	Symmetric stretching vibration of CH_2
2878	Asymmetric stretching vibration of CH_2
2934	Symmetric stretching of the CH_3 moiety
1125/1080	Ordered lipid distribution
2878/2934	Lipid/protein

University, and for each patient, a boundle of hair fibers were collected and examined. The normal hair for comparison was obtained from three healthy persons in our institute. All hair was cut at 1 cm length from the root on the scalp. As melanin of the black hair has strong absorption to the incident light, white hair was chosen for Raman experiments.

The hair was washed with a 10% (w/w) sodium lauryl ether sulphate solution followed by distilled water rinsing about 30 s to remove any surface contamination and then dried in air. The hair fibers were then embedded in the OCT (Optical Cutting Tool), and then immediately frozen in −22 °C. The frozen tissue was cross-cut by a microtome into 40 μm thick sections and was then floated on the quartz plate for Raman measurements.

2.2. Raman microspectroscopy and imaging measurements

The Raman experiment was conducted using XploRA (HORIBA) Raman spectrometer which is equipped with four gratings (namely, 600/mm, 1200/mm, 1800/mm and 2400/mm) and two lasers (i.e., the 532 nm laser and the 785 nm laser). In this work, the 600/mm grating and the 785 nm laser were employed. The laser power was below 2.5 mW to avoid local sample heating. The scanning platform was automatically controlled by the motor which has the minimal mechanical step 0.1 μm. For the Raman imaging measurement, the scanning step in the *X* direction was 1.5 μm and the step in the *Y* direction was 1.5 μm. The spectral resolution is ca. 4 cm^{-1}. For the scanning, the Raman spectra were taken from single points in the cross-sections of the hair fibers.

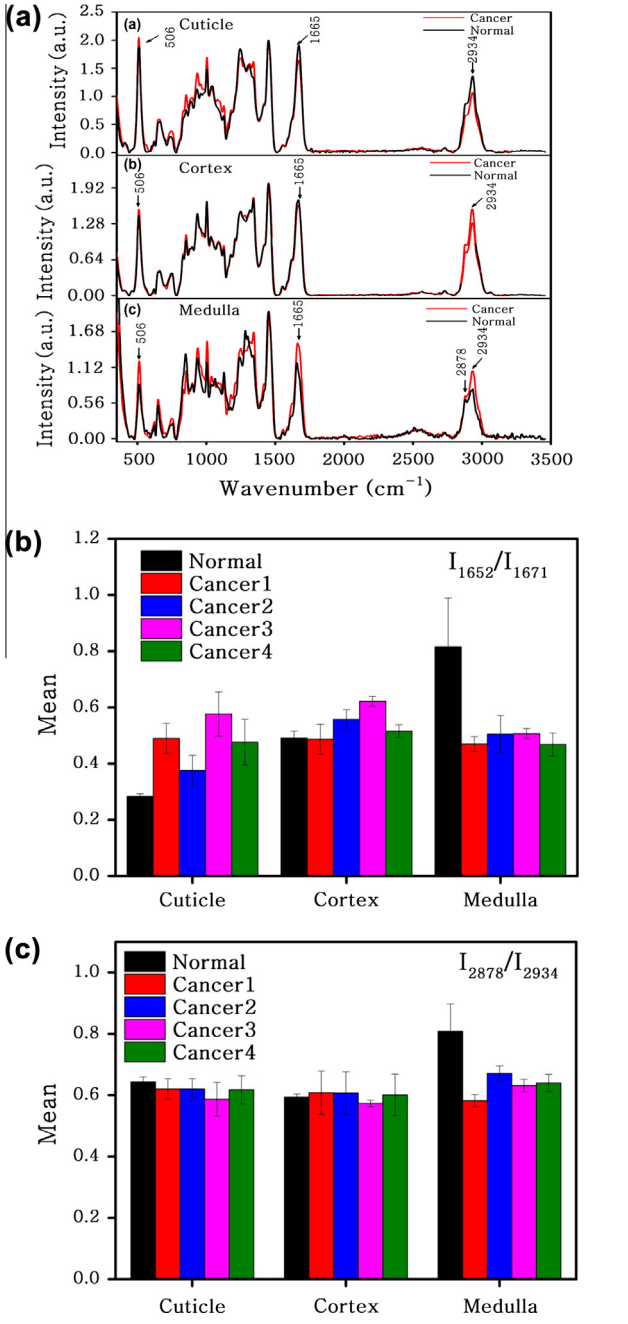

Fig. 3. (a) Single-point Raman spectral comparison between the cancer patients' hair and normal hair. (b) Spectral analysis for comparing the relative content α-helix to β-sheet structures in three different regions of the hair from cancer patients, and (c) spectral analysis for comparing the relative content of lipid in the three sections of hair from cancer patients.

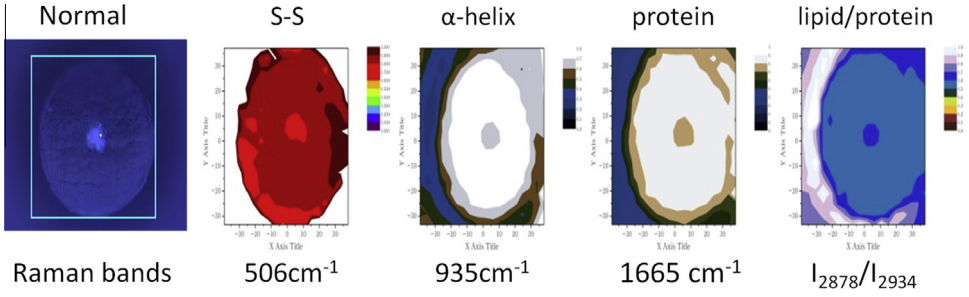

Fig. 2. Raman imaging of cross-section of the normal hair. Height of peak used as parameter for chemical mapping. Color bar from the bottom to the top represents quantity of chemical composition increases. The imaging plots visually illustrate that the cuticle of normal hair contains more disulfide conformers but less α-helix structures, while the medulla contains more lipid but less disulfide conformers.

As for the spectral data treatment for hair analysis and comparison, all the measured spectra were processed with baseline subtraction followed by intensity normalization at 1450 cm^{-1}. The Raman signal from OCT around the hair fiber was weak enough so that it could be ignored in spectral analysis. The Raman mapping plots were depicted using Origin program.

3. Results and discussion

3.1. Establishment of reliable spectral analysis approach tesified by the assessment of the normal hair from healthy people

First of all, it is required to establish the reliable method for analyzing the hair spectral data correctly. For this purpose, the normal hair from healthy people was tested at first and compared with the results in the literature.

As already known, human hair is normally divided into three different sections, i.e., cuticle, cortex and medulla [15]. Fig. 1a shows the Raman spectra from the hair from normal healthy people, with the measuring points taken from the three sections of the hair and the spectra normalized at 1450 cm^{-1} (assigned to $\delta(CH_2)$ vibration) for comparison. The assignments of Raman bands of hair [15–22] is given in Table 1. The histograms in Fig. 1b illustrate the differences in chemical compositions for three different sections. Obviously, the intensity of the band at 506 cm^{-1} (S–S stretching vibration) decreases successively from cuticle to medulla, confirming that cuticle contains maximal concentration of disulfide conformers (because of more keratin in cuticle). On the contrary, the intensity of the band at 935 cm^{-1} (α-helix protein C–C skeleton stretching vibration [16]) in medulla is relatively higher, indicating that more α-helix structured proteins are distributed in medulla. Also, the Amide I band in medulla and cortex moves to lower wavenumber, verifying that there are more α-helix proteins distributed in the cortex and medulla regions. The medulla also has the higher intensity at 2878 cm^{-1} (asymmetric stretching vibration of $-CH_2$ from lipid [15]), but lower intensity at 2934 cm^{-1} (symmetric stretching vibration of $-CH_3$ from protein [15]), so the intensity ratio $I(2878\ cm^{-1})/I(2934\ cm^{-1})$ (lipid/protein) [15] is the largest in medulla, indicating that the medulla contains higher concentration of lipid than cuticle and cortex. Moreover, the Amide I analysis [22] (as shown in Figs. S2 and S3 in Supplementary Information) delivers the same information.

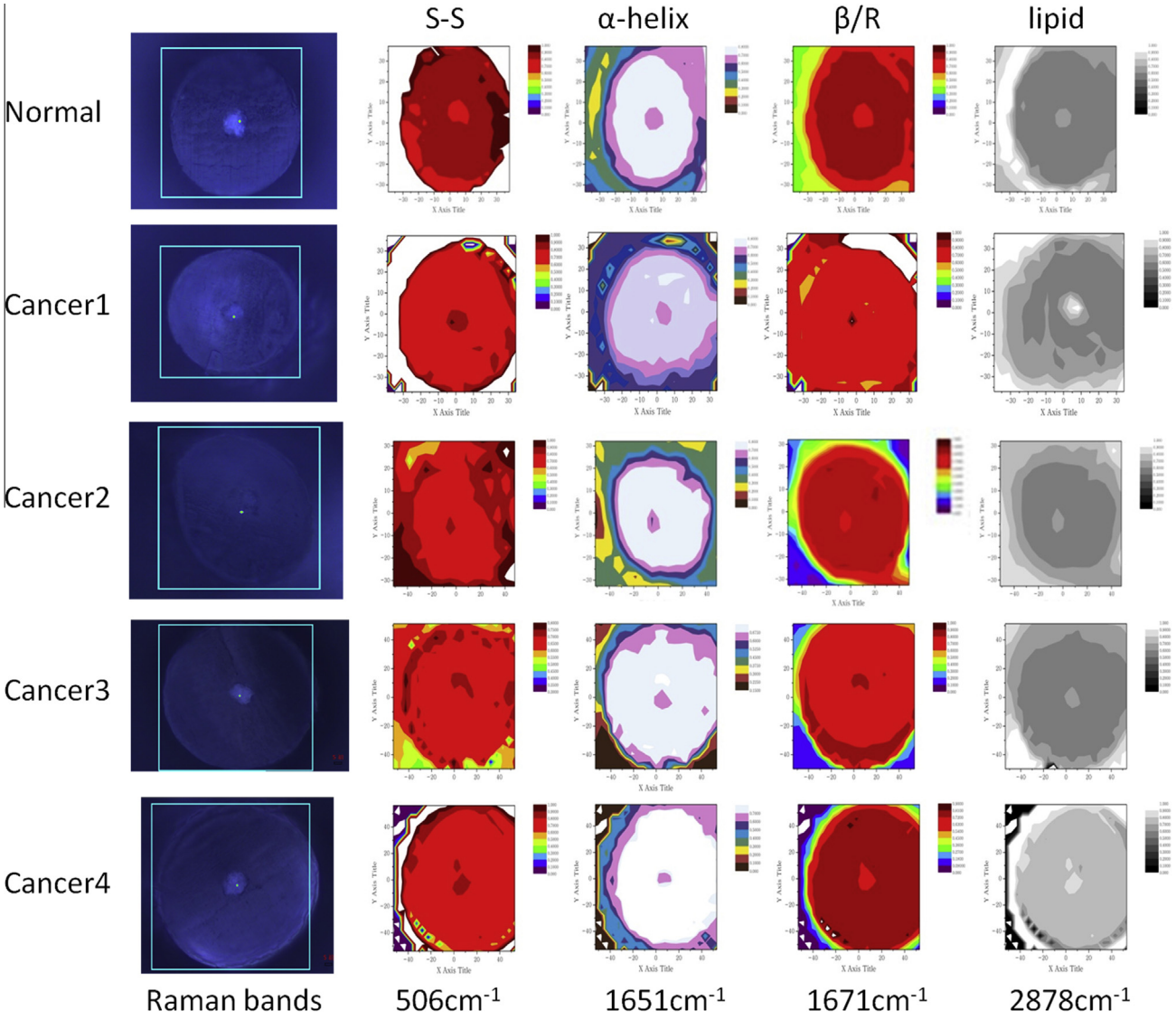

Fig. 4. Raman imaging of the hair from cancer patients in contrast with the the normal hair from healthy people. Overall, it shows that in the medulla of the cancer patients' hair has less percentage of α-helix structures but more lipid than the cortex of hair.

Fig. 2 shows the Raman imaging plots of the normal hair. It illustrates the details of the chemical distribution with spatial resolution, further confirming the above conclusions, i.e., the cuticle contains more disulfide proteins but less α-helix structured proteins than cortex and medulla, while the medulla contains higher ratio of lipid to protein than other sections of the normal hair.

All these results are consistent with the literatures [15,16], confirming that our Raman measurements together with the analysis approach are appropriate and reliable.

3.2. Comparison of the hair from rectum cancer patients with the hair from normal people

Fig. 3 shows the comparison between the cancer patients' hair and the normal hair. In the cuticle, there is little difference for the 506 cm^{-1} band, suggesting that the growth of keratin in the cuticle does not vary significantly among different people. In the cortex, the intensity at 1665 cm^{-1} is weaker in the cancer case, implying that the cancer patients' hair may contain overall less proteins. In the medulla, the intensity at 1665 cm^{-1} are significantly greater, and the Amide I band moves to the higher frequency, indicating that the medulla of the cancer patients' may have higher concentration of non-helical structures.

Further spectral comparison based on the analysis of Amide I band (1652/1671 cm^{-1}) and lipid/protein band (2878/2934 cm^{-1}) is given in Fig. 3b and c, illustrating the following results: (a) in cuticle and cortex, the cancer patients' hair has similar composition of α-helix proteins compared with normal hair; (b) the medulla of the cancer patients' hair contains less α-helix but more β-sheet/R (R denotes for random coiled structrure) structures; and (c) the cancer patients' hair contains higher concentration of lipid in the medulla than normal hair.

Therefore, significant differences exist mainly in the medulla region. In contrast with normal hair, the medulla in the cancer patients' hair contains higher concentration of non-α-helix structures but lower ratio of lipid to proteins. While the underlying physiological reason is still elusive, this observation is similar to the result obtained from FTIR-spectroscopy [23,24]. Obviously, the rectal cancer disease affect the hair growth process significantly.

Fig. 4 shows the Raman imaging comparison between the hair from the cancer patients and the hair from normal people. With more detailed spatial information, it just confirms the conclusion as obtained from the analysis based on the single point spectra.

4. Conclusion and remarks

Based on Raman microspectroscopy and imaging, the difference between the rectum cancer hair and normal hair has been identified. While our Raman analysis of normal hair consists with the previous work reported in the literature, the newly observed spectral difference as revealed by comparison between the hair from rectal cancer patients and the hair from healthy persons suggests that Raman microspectroscopy and imaging may be employed for cancer diagnosis. For example, it shows that in the rectal cancer patients' hair, the medulla contains higher density of lipid but lower density of α-helix proteins. Although this study is still preliminary, it is however a first demonstration for applying the method of Raman microspectroscopy and imaging technique to analyze non-cancer tissues such as human hair for possible and convenient medical diagnosis of cancers.

Acknowledgments

This work was supported by the One-hundred-Talent Program of the Chinese Academy of Sciences. We also would like to thank Mr. Dake Huang for the assistance in preparation of hair samples.

Appendix A. Supplementary material

Supplementary data associated with this article can be found, in the online version, at http://dx.doi.org/10.1016/j.molstruc.2013.05.005.

References

[1] R.J. Swain, M.M. Stevens, Biochem. Soc. Trans. 35 (2007) 544.
[2] P. Chen, A. Shen, X.D. Zhou, J. Hu, Anal. Methods 3 (2011) 1257.
[3] H. Abramczyk, B. Brozek-Pluska, J. Surmacki, J. Jablonska-Gajewicz, R. Kordek, Prog. Biophys. Mol. Biol. 108 (2012) 74.
[4] H. Abramczyk, B. Brozek-Pluska, J. Surmacki, J. Jablonska, R. Kordek, J. Mol. Liq. 164 (2011) 123.
[5] G.J. Pupples, J. Greve, R.J.H. Clark, Biomed. Appl. Spectrosc. 1 (1996) 1.
[6] C.X. Yu, E. Gest, K. Eckert, D. Allara, J. Irudayaraj, Cancer Detect. Prevent. 30 (2006) 515.
[7] B.W.D. de Jong, T.C. Bakker Schut, J. Coppens, K.P. Wolffenbuttel, D.J. Kok, G.J. Puppels, Vib. Spectrosc. 32 (2003) 57.
[8] R.O.P. Draga, M.C.M. Grimbergen, P.L.M. Vijverberg, C.F.P. van Swol, T.G.N. Jonges, J.A. Kummer, J.L.H.R. Bosch, Anal. Chem. 82 (2010) 5993.
[9] P. Crow, B. Barrass, C. Kendall, M. Hart-Prieto, M. Wright, R. Persad, N. Stone, Br. J. Cancer 92 (2005) 2166.
[10] T.J. Harvey, A. Henderson, E. Gazi, N.W. Clarke, M. Brown, E. Correia Faria, R.D. Snook, P. Gardner, Analyst 132 (2007) 292.
[11] C.M. Krishna, G.D. Sockalingum, B.M. Vadhiraja, K. Maheedhar, A.C.K. Rao, L. Rao, L. Venteo, M. Pluot, D.J. Fernades, M.S. Vidyasgar, V.B. Kartha, M. Manfait, Biopolymers (2007) 85214.
[12] H.G.M. Edwards, N.F.N. Hassan, A.S. Wilson, Analyst 129 (2004) 956.
[13] C. Liang, A. Morris, S. Schlucker, K. Imoto, V.H. Price, E. Menefee, S.M. Wincovitch, I.W. Levin, D. Tamura, K.R. Strehle, K.H. Kraemer, J.J. DiGiovanna, J. Invest. Dermatol. 126 (2006) 2210.
[14] K. S Kim, J. Lee, Min-hyung Jung, Y. J Choi, Hun-Kuk Park, Microsc. Res. Tech. 74 (2011) 1121.
[15] G.J. Zhang, L. Senak, D.J. Moore, J. Biomed. Opt. (2011) 16.
[16] S. Schlücker, K.R. Strehle, J.J. DiGiovanna, K.H. Kraemer, I.W. Levin, Biopolymers (2006) 82615.
[17] A. Kuzuhara, N. Fujiwara, T. Hori, Biopolymers 87 (2007) 134.
[18] C.H. Xiao, C.R. Flach, C. Marcott, R. Mendelsohn, Appl. Spectrosc. 58 (2004) 382.
[19] R. Mendelsohn, Biochim. Biophys. Acta – Biomembr. 290 (1972) 15.
[20] P. Dhamelincourt, F.J. Ramirez, Appl. Spectrosc. 47 (1993) 446.
[21] J.S. Church, G.L. Corino, A.L. Woodhead, Biopolymers 42 (1997) 7.
[22] A. Kuzuhara, Biopolymers 77 (2005) 35.
[23] X. Wang, Z.M. Qi, X.C. Liu, S.Y. Wang, C.X. Li, G. Liu, Y. Xiong, T.T. Li, J.Q. Tao, Y.C. Tian, Cancer Epidemiol. 34 (2010) 453.
[24] D.J. Lyman, J.M. Wijelath, Appl. Spectrosc. 59 (2005) 26.